PHYSICAL REVIEW A VOLUME 31, NUMBER 3 MARCH 1985

Mass and dimension of Feigenbaum attractors

Simon Fraser and Raymond Kapral
Department of Chemistry, University of Toronto, Toronto, Ontario, Canada M5S 1A1
(Received 10 August 1984)

Attractor structure on the real line is represented as a mass function $M(x)$ defined as the fraction of attractor points to the left of x. For Feigenbaum attractors, M is a devil's staircase which possesses both orbit and mass scaling features. The attractors $\mathscr{A}_p$ for maps with a pth-order extremum are discussed in terms of this scaling, which leads to a hierarchy of bounds for the corresponding mass M_p. Both $\mathscr{A}_p$ and M_p transform in a characteristic way under power-law conjugacy; this gives rise to two kinds of global scaling. A further intermediate scaling for the quartic attractor which underlies vector scaling in two-extremum maps is discussed in this context. As p tends to infinity, the capacity dimension D tends to 1 and the information dimension σ to 0. The effects of this trend on the appearance and observability of attractors are discussed.

I. INTRODUCTION

One of the most studied chaos-producing mechanisms involves an infinite cascade of subharmonic bifurcations resulting in an aperiodic orbit. Quantitative investigations on the nature of the chaotic attractor are usually carried out through studies of the properties of discrete-time maps, extracted from the flow by various techniques. These maps typically possess quadratic extrema and it is the quadratic character of the extremum that determines many of the attractor's properties, such as its scaling features[1] and its dimension.

Although the (Feigenbaum) attractors which appear at the subharmonic cascade limit are not generic, i.e., they are replaced by finite or banded attractors under small parameter perturbations, their structure governs empirical estimates of dimension at finite resolution in the parameter-space neighborhood that contains them. This is so because finite (orbit) scaling imitates its fractal limit, thus, these attractors acquire greater practical importance.

The attractors associated with maps having (differentiable) nonquadratic extrema have been less well studied but they do arise in physical problems. It is not necessary that a map derived from a flow explicitly exhibit a nonquadratic extremum since the interaction of several lower-order extrema can yield behavior characteristic of a higher-order extremum. Examples are provided by the Rössler flow[2] near the transition from spiral to screw chaos[3,4] and the circle and related maps above criticality.[5,6] In both cases the maps have two quadratic extrema and quartic scaling behavior is observed in part of the parameter plane. Interaction of more extrema (as for the Rössler flow in the screw-chaos region) can give rise to yet higher-order scaling behavior. These observations have stimulated the present investigation on the nature of the Feigenbaum attractors arising from maps with a pth-order extremum.

The organization of the paper is as follows. In Sec. II we discuss the scaling properties of the attractor through a study of its "mass" curve $M_p(x)$, i.e., the fraction of points on the attractor lying on a specified x-dependent interval. Scaling exponents for the centers and edges of the attractor clusters on $M_p(x)$ are introduced and global attractor scaling is defined in terms of these exponents. In Sec. III $M_p(x)$ for $p=4$ is examined since this produces a new scaling (under power-law conjugacy) which underlies the behavior of two-parameter maps. The structure of the attractors for arbitrarily large p is considered in Sec. IV. The orbit scaling factor α and its powers are shown to play a central role: they are directly related to formulas for the capacity and information dimensions. The singular limit $p=\infty$ is examined in the context of mass distribution and dimension. Finally, we discuss the experimental and theoretical implications of our work in Sec. V.

II. MASS CURVE AND ITS SCALING PROPERTIES

We investigate the structure of the Feigenbaum attractors $\mathscr{A}_p$ arising from map functions with a single pth-order extremum. A quantitative, global, scaling theory for such attractors may be developed by considering the functions $g_p(|x|^p)$, which obey the doubling transformation[1]

$$g_p(x)=\alpha_p g_p(g_p(x/\alpha_p)) \ . \tag{2.1}$$

The attractor associated with g (Ref. 7) will be denoted by $\mathscr{A}_p(g)$; it possesses exactly self-similar scaling features at all levels of its Cantor-set structure. Clusters of points in $\mathscr{A}_p(g)$ scale by α at the origin and its preimages and by α^p at images of the origin due to the focusing effect of the extremum. Since the orbit itinerary is independent of p (if g_p has only one extremum), the basic organization of these attractors is the same for all p.

The structure of the attractor is conveniently discussed using the decimation scheme of Grassberger.[8] Starting from the origin $x_0=0$ and defining $x_{j+1}=g(x_j)$ one may easily deduce the scaling relation $x_{2j}=\alpha^{-1}x_j$. Furthermore, for all odd j, $x_j>0$. A number of properties follow from the itinerary starting from the origin: letting $\mathscr{A}_{i,j}=\mathscr{A}_p[x_i,x_j]$ be the attractor on $[x_i,x_j]$ we observe that the entire attractor is $\mathscr{A}_{2,1}$ and that

$\mathscr{A}_{2,1}=\mathscr{A}_{2,4}\cup\mathscr{A}_{3,1}$. Also (formally) $\mathscr{A}_{2,4}=\alpha^{-1}\mathscr{A}_{2,1}$ and $\mathscr{A}_{2,4}=g(\mathscr{A}_{3,1})$. Repetition of this argument permits the construction of sets of exactly self-similar attractor fragments (see the inset of Fig. 1).

Certain aspects of the attractor's structure are revealed by examination of its mass curve, which we define as

$$M_p(x)\equiv M(x;\mathscr{A}_p(g)) , \tag{2.2}$$

the fraction of points of $\mathscr{A}_p(g)$ contained in $[g(1)=\alpha^{-1},x]$. This function has the form of a "devil's staircase," which increases continuously on the set $\mathscr{A}_p$ and clearly exhibits many of the scaling properties of $\mathscr{A}_p$. A graph of $M_2(x)$ is shown in Fig. 1. Several features of this curve hold for all mass curves $M_p(x)$. The clusters on $\mathscr{A}_2$ are represented by steps on $M_2(x)$ and cluster scaling by α^{-1} in width and 2^{-1} in height is evident in the figure. The cluster width scaling is the same as the scaling of $\mathscr{A}_2$ at $x=0$ and its preimages.

The distribution of mass on $\mathscr{A}_p$ follows directly from the decimation procedure for constructing the attractor. In particular, we may show that mass to the left of the origin is $\frac{1}{3}$ while that to the right is $\frac{2}{3}$ (cf. the Appendix).

Self-similar features on $M_p(x)$ may be located by bounding curves through the point $(x=0,M=\frac{1}{3})$ in the (x,M) plane. Referring to Fig. 1 for $M_2(x)$ the right-hand upper bound $B_R(x)$ to $M_2(x)$ obeys the constraints

$$M(\alpha^{-2j})-M(0)=B_R(\alpha^{-2j})-\tfrac{1}{3}=2^{1-2j}/3 \quad (j=0,1,\ldots) , \tag{2.3}$$

which are just the conditions for the touching of $B_R(x)$ and $M(x)$ at the points $x=\alpha^{-2j}$. Letting j be continuous and $x=|\alpha|^{-2j}$ we find

$$B_R(x)=\tfrac{1}{3}+\tfrac{2}{3}|x|^{\eta_c} , \tag{2.4}$$

with

$$\eta_c=\ln 2/\ln|\alpha| . \tag{2.5}$$

Near $x=0$, $B_R(x)$ touches $M(x)$ infinitely often. Curves with the same exponent η_c but different amplitudes $(\neq\frac{2}{3})$ connect other sets of self-similar features on M. Along with $B_R(x)$, three other universal bounds emanating from this origin confine $M(x)$:

$$\begin{aligned} b_R(x)&=\tfrac{1}{3}+\tfrac{1}{6}[g^{(3)}(0)]^{-\eta_c}|x|^{\eta_c} ,\\ b_L(x)&=\tfrac{1}{3}-\tfrac{2}{3}|x|^{\eta_c} ,\\ B_L(x)&=\tfrac{1}{3}-\tfrac{1}{6}[g^{(3)}(0)]^{-\eta_c}|x|^{\eta_c} . \end{aligned} \tag{2.6}$$

Here b refers to a lower bound and B to an upper bound while L and R denote bounding curves to the left and right of the origin, respectively. This global center scaling is imitated by a local scaling about the centers (preimages of the origin) of clusters on the attractor.

We have just presented the standard description of global attractor scaling about the origin when the universal function g possesses a pth-order extremum there. A complementary global theory exists for attractor scaling about cluster edges using power-law conjugacy.

We define functions $h_q(x)$ and $h_q^{-1}(x)$ by[9]

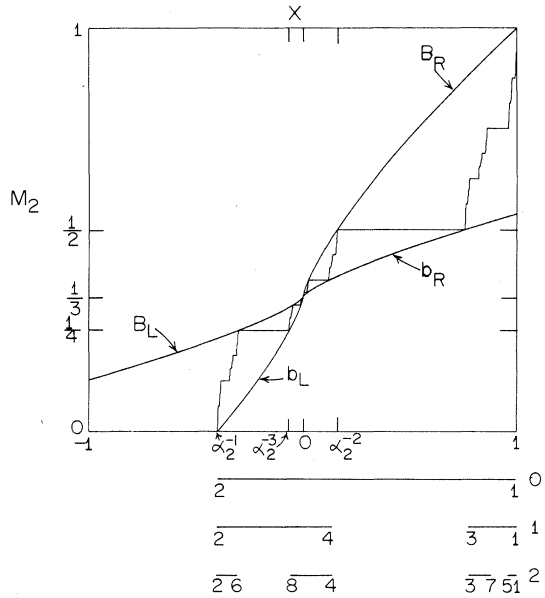

FIG. 1. Top part of the figure shows the mass curve $M_2(x)=M(x;\mathscr{A}_2)$. Center bounds $b_{L,R}$ (lower) and $B_{L,R}$ (upper) to the left (L) and right (R) of the origin 0 depend on quadratic exponent η_c (see text) and indicate global scaling of M_2 about 0. Bounds meet the point $(x=0,M=\frac{1}{3})$ with infinite derivative. Labeling of axes indicates scaling of cluster masses by 2^{-1} and distances by α_2^{-1}. Bottom part of the figure shows the decimation of the interval $[\alpha_2^{-1},1]$ generated by the trajectory $x_0=0$, $x_1=1,\ldots,x_j$. Numbers 0,1,... are indices j. At the nth level of decimation 2^n new points define the excised intervals (see text).

$$h_q(x)=x^{1/q} \tag{2.7}$$

and

$$h_q^{-1}(x)=x^q . \tag{2.8}$$

Then there is a power-law conjugate universal function $\mathscr{P}_q g_p$ of g_p defined by

$$\mathscr{P}_q g_p\equiv h_q^{-1}\circ g_p\circ h_q , \tag{2.9}$$

which obeys the doubling transformation [Eq. (2.1)] with scale factor α_p^q, i.e.,

$$\mathscr{P}_q g_p(x)=\alpha_p^q\,\mathscr{P}_q g_p(\mathscr{P}_q g_p(x/\alpha_p^q)) . \tag{2.10}$$

Let $\mathscr{A}_{p/q}$ denote the attractor of $\mathscr{P}_q g_p$. (In this notation $\mathscr{A}_p\equiv\mathscr{A}_{p/1}$.) Taking $q=p$ we see that $\mathscr{P}_p g_p$ is a function which behaves like $1+C|x|$ at the origin and $|\delta x|^p$ at the conjugate image of the zero of g_p (in [0,1]). $\mathscr{P}_p g_p$ looks like an inverted, reflected version of g_p. Geometrically, $x=1$ in g_p corresponds to $x=0$ in $\mathscr{P}_p g_p$, so the origin becomes the edge of the attractor $\mathscr{A}_{p/p}$ and the extremum of $\mathscr{P}_p g_p$ is mapped into the origin in one step. Because $\mathscr{P}_p g_p$ obeys the doubling transformation the attractor $\mathscr{A}_{p/p}$ possesses global edge scaling by α_p^p about $x=0$. Edge scaling is obeyed locally for $\mathscr{P}_p g_p$ at the im-

ages of the origin (cf. center scaling for g_p).

This functional and attractor scaling corresponds to a scaling law for the mass M: for even integer $q<p$ the formal transformation from $\mathscr{A}_p$ to $\mathscr{A}_{p/q}$ can be written $\mathscr{A}_{p/q}=h_q^{-1}(\mathscr{A}_p)$, which can be restated in terms of attractor elements. Starting from $x_0=0$ under $g_p(x)$, and $\xi_0=0$ under $\mathscr{P}_p g_p$, the g_p time series $\{x_j\}$ and the $\mathscr{P}_q g_p$ time series $\{\xi_j\}$ are related by $\xi_j=|x_j|^q$. The transformation of the mass curve ($M_p\to M_{p/q}$) under power-law conjugation follows from this relation. The mass of $\mathscr{A}_p$ on $[-x,x]$ is equal to the mass of $\mathscr{A}_{p/q}$ on $[0,\xi]$ giving

$$M_{p/q}(\xi)=M_p(\xi^{1/q})-M_p(-\xi^{1/q})\ . \tag{2.11}$$

For $q=p$ this becomes

$$M_{p/p}(\xi)=M_p(\xi^{1/p})-M_p(-\xi^{1/p})\ . \tag{2.12}$$

The mass $M_{2/2}$ for the quadratic attractor $\mathscr{A}_{2/2}$ is shown in Fig. 2. Since scaling at the origin of $\mathscr{A}_2$ goes as α_2, scaling at the origin of $\mathscr{A}_{2/2}$ goes as α_2^2.

Consider M_p for a moment: assuming that the mass at the origin behaves as $|x|^{\eta_c}$, use of the Perron-Frobenius equation leads to an edge-scaling exponent $\eta_e=\eta_c/p$. The exponent η_e corresponds to the scale factor α_p^p in the doubling transformation. However, this local relation is globally true for $\mathscr{P}_p g_p$ where the attractor edge appears at $x=0$. Figure 2 shows the corresponding global bounds b_0 and B_0 for $\mathscr{P}_2 g_2$, which emanate from the origin with infinite derivative corresponding to the edge (origin) exponent $\eta_e=\eta_c/2$.

The upper B_0 and lower b_0 bounds are given by

$$\begin{aligned} B_0(x)&=|x|^{\eta_e}\ ,\\ b_0(x)&=\tfrac{1}{2}\,|\mathscr{P}_2 g_2(|\alpha|^{-2})|^{-\eta_e}\,|x|^{\eta_e}\ . \end{aligned} \tag{2.13}$$

The amplitude for b_0 in Eq. (2.13) is the case $p=q=2$ of the general formula for this quantity, i.e., $\frac{1}{2}\,|\mathscr{P}_q g_p(|\alpha|^{-q})|^{-\eta_e}$.

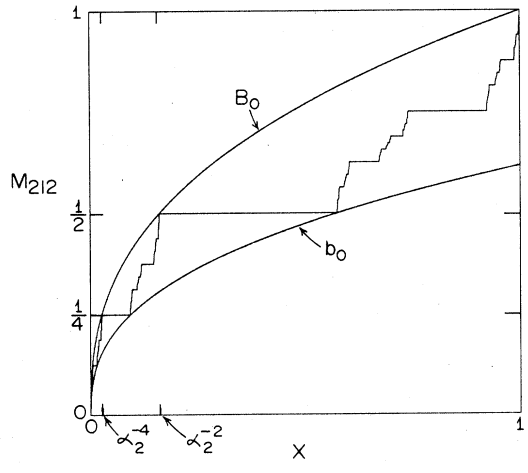

FIG. 2. Mass curve $M_{2/2}=M(x;\mathscr{A}_{2/2})$ corresponding to global edge scaling by α_2^2. The bounds b_0 and B_0 to $M_{2/2}$ depend on the quadratic edge exponent $\eta_e=\frac{1}{2}\eta_c$. The bounds meet at $(x=0,M=0)$ with infinite derivative. $M_{2/2}$ contains cluster scaling in mass by 2^{-1} and distance by α_2^{-2} as indicated by the axis labeling.

Just as M_2 touches the global bounds $B_{L,R}$ and $b_{L,R}$ infinitely often near $x=0$, so $M_{2/2}$ touches b_0 and B_0 infinitely often there also. From Fig. 2, on the curve $M_{2/2}$ the principal clusters within $\mathscr{A}_2$ itself scale in width and separation from the origin by α^{-2} and in height by 2^{-1}. This one-sided edge scaling follows automatically from the appearance of α^2 in the global scaling law, i.e., Eq. (2.10). A similar statement with α_2^{-1} replacing α_2^{-2} describes the global scaling in Fig. 1, where attractor fragments appear on both sides of the origin since $\alpha_2<0$. These global scalings are of course reflected in the local edge and center scaling of the asymptotically self-similar clusters in either $\mathscr{A}_2$ or $\mathscr{A}_{2/2}$.

Because of the geometrical inversion of $\mathscr{P}_2 g_2$ with respect to g_2, on $\mathscr{A}_{2/2}$ $\frac{1}{3}$ of the mass lies to the right of the extremum of $\mathscr{P}_2 g_2$ and $\frac{2}{3}$ to the left; denoting the preimage of $x_0=0$ by x_{-1} (the zero of g_2) we therefore have for $\mathscr{A}_2$ the mass distribution

$$M[\alpha^{-1},0]=M[0,x_{-1}]=M[x_{-1},1]=\tfrac{1}{3}\ . \tag{2.14}$$

While the attractors $\mathscr{A}_2$ and $\mathscr{A}_{2/2}$ are not geometrically identical they are very similar: "almost global" edge bounds exist for $\mathscr{A}_2$ and almost global center bounds exist for $\mathscr{A}_{2/2}$.

Grassberger[10] has recently noted that generalized dimensions which may be used to characterize the attractor are invariant under conjugation by differentiable, invertible maps. Power-law conjugacy possesses this property except at the origin. Thus, for general $q\le p$, the attractors $\mathscr{A}_2$ and $\mathscr{A}_{2/2}$ have exactly the same dimensions as we have verified by calculation. Hence, distinct p-type attractors $\mathscr{A}_p$, $\mathscr{A}_{p/q}$, etc. belong to the same equivalence class with respect to the entire set of their dimensions, which, therefore, does not distinguish or completely characterize them.

III. MASS CURVE FOR THE QUARTIC ATTRACTOR

We devote this section to a study of the properties of the quartic attractor, as reflected in its mass curve, in view of its relevance to a number of dynamical systems.

The functions g_4, obeying Eq. (2.1) and $\mathscr{P}_4 g_4$, obeying (2.10) with $p=q=4$, give rise to attractors $\mathscr{A}_4$ and $\mathscr{A}_{4/4}$ with the respective mass curves M_4 and $M_{4/4}$. These two quartic attractors correspond directly to the quadratic attractors $\mathscr{A}_2$ and $\mathscr{A}_{2/2}$ discussed above. M_4 ($\equiv M_{4/1}$) shown in Fig. 3(a) possesses global center scaling with exponent $\eta_c=\ln 2/\ln|\alpha_4|\approx 1.3205$. Since $\eta_c>1$ the bounds $B_{L,R}$ and $b_{L,R}$ emanate from the origin with zero slope.[11] $M_{4/4}$ given by Eq. (2.12) with $p=q=4$ is shown in Fig. 3(b), it is a folded, scaled version of M_4; the edge exponent $\eta_e=\ln 2/4\ln|\alpha_4|\approx 0.3301$ governs the (quartic) bounds b_0 and B_0 through $x=0$ that confine $M_{4/4}$. Attractor and mass scaling under g_4 and $\mathscr{P}_4 g_4$ are formally similar; on $M_{4/q}$ ($q=1$ or 4) the principal $\mathscr{A}_4$ component clusters scale in height by 2^{-1} and in width and separation from the origin by α_4^{-q} as shown in Figs. 3(a) and 3(b). (In Ref. 12 g_4 was called q_4.) Like the quadratic case the hierarchy of subclusters of $\mathscr{A}_{4/q}$ scale asymptoti-

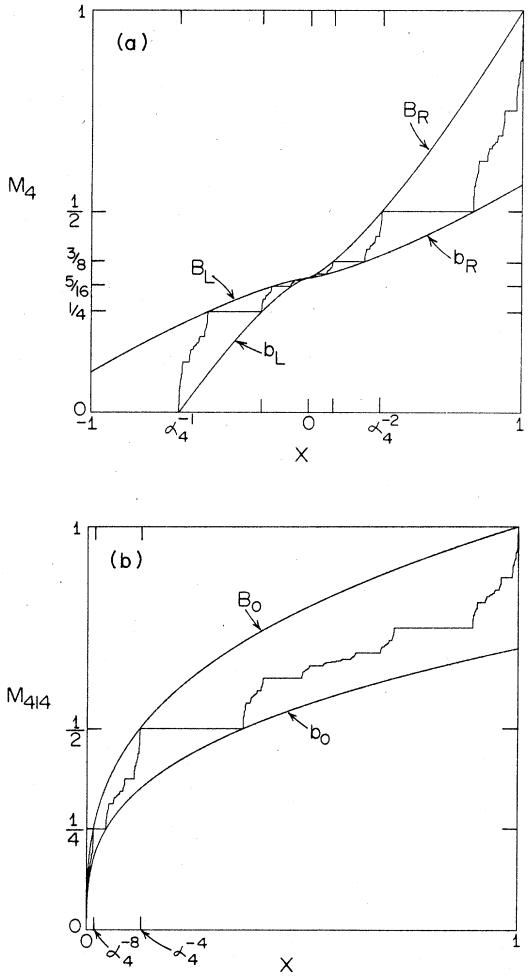

FIG. 3. (a) $M_4(x)$ (cf. Fig. 1). Scaling clusters on left ($x \leq 0$) of masses $\frac{1}{4}, \frac{1}{16}, \ldots$ are matched with (inverted) clusters on right ($x \geq 0$) with masses $\frac{1}{2}, \frac{1}{8}, \ldots$ (see ordinate M) as described in text. Note scaling of cluster distances by α_4^{-1}. Left and right clusters meet at ($x=0, M=\frac{1}{3}$). Global bounds $b_{L,R}$ and $B_{L,R}$ are labeled as in Fig. 1; they meet at ($x=0, M=\frac{1}{3}$) with zero derivative. (b) Mass curve $M_{4/4}=M(x;\mathscr{A}_{4/4})$ with edge-scaling property is shown (cf. Fig. 2). Bounds b_0 and B_0 dependent on quartic edge exponent η_e indicate global scaling of mass. Clusters on $M_{4/4}$ scale in height (mass) by 2^{-1} and distance by α_4^{-4} as indicated by labeling of axes.

cally like $\mathscr{A}_4$ with respect to their centers (preimages of $x=0$) and edges (images of $x=0$).

However, for the quartic attractor another (natural) possibility arises from power-law conjugation, namely $p=4$ and $q=2$ so $p/q=2$. This gives the universal function $\mathscr{P}_2 g_4$ with scale parameter α_4^2 about the origin. (In Ref. 12 $\mathscr{P}_2 g_4$ was called q_2 and α_4^2 was α_2.) Functions like $\mathscr{P}_2 g_4$ appear frequently in physical applications where quartic behavior results from an underlying map possessing two interacting quadratic extrema, where a single step links the extrema. In particular, we have previously carried out a detailed study of the sine map $x_{t+1}=x_t+a+b\sin(2\pi x_t)$, which displays quartic behavior along certain lines in the (a,b) plane. Maps with two such interacting extrema actually exhibit more complicated vector-scaling features:[12,13] there are two relevant vectors in the renormalization-group theory.

The properties of $\mathscr{P}_2 g_4$ are formally like those of the other quartic universal functions and the local cluster scaling of $\mathscr{A}_{4/2}$ shows the features present in $\mathscr{A}_4$ and $\mathscr{A}_{4/4}$. However, the origin possesses a new, intermediate exponent $\eta_0=\ln 2/2\ln|\alpha_4|$ corresponding to the global scaling by α_4^{-2} about $x=0$ and the appearance of α_4^2 in the doubling transformation [Eq. (2.10)] for $\mathscr{P}_2 g_4$. Because a single step links the minimum of $\mathscr{P}_2 g_4$ to its maximum at $x=0$ (global) scaling by α_4^2 appears only at the origin in $\mathscr{P}_{4/2}$ and not at any image or preimage of this point. The corresponding mass $M_{4/2}$, which is related to M_4 by Eq. (2.11) with $p=4$, $q=2$, is shown in Fig. 4. Thus the main $\mathscr{A}_4$ clusters on $M_{4/2}$ scale in height by 2^{-1} and in width and separation from $x=0$ by α_4^{-2}.

This separation of dynamically quartic behavior into contributions from two quadratic extrema, in $\mathscr{P}_2 g_4$ for example, underlies the vector scaling mentioned earlier. In two-parameter, multiextremum maps many steps may link any two extrema; in the parameter plane the number of such iterates labels the branches and end vertices (tricritical points) of an infinite binary tree of subharmonic cascades.[12] On the infinitely bifurcated orbits associated with tricritical points the first extremum visited supports $\mathscr{A}_4$ locally and all iterates along the link including its terminus support $\mathscr{A}_{4/2}$ locally. (The function $\mathscr{P}_2 g_4$ provides the simplest case of this global structure.) Each $\mathscr{A}_{4/2}$ possesses one α_4^2-scaling end vertex, which is an element of the link. Finer $\mathscr{A}_4$-like fragments are of course embedded in the main clusters along the link.

Just as two quadratic extrema produce quartic behavior, three coupled quadratic extrema produce octic behavior, potentially a co-dimension-3 scenario. (However, conjugation at two origins is required to decompose an octic into three quadratic extrema.) Thus coupling extrema is an important mechanism whereby high-order behavior may be built up in both maps and flows.

IV. MASS AND DIMENSION OF ATTRACTORS FOR ARBITRARY p

The structure of the attractors for arbitrary p was studied by considering the class of functions

$$f_p(x)=1+a|x|^p \quad (p>0,\ a<0)\ . \tag{4.1}$$

The dependence of α and δ on p is shown in Table I, which extends previous results.[14–18] These data were obtained empirically from the scaling properties of the superstable subharmonic orbits as a tends to a_∞, the value of a at the subharmonic limit. The results strongly suggest that $|\alpha|\to 1$ and $\delta\to\infty$ as $p\to\infty$.

The decrease in $|\alpha|$ results in a rise in the center exponent η_c and produces a flattening of the mass M_p in the middle of the interval $[\alpha^{-1},1]$ which contains the at-

TABLE I. Data for the first subharmonic limit (period 2^∞) for functions $f_p(x)=1+a\,|x|^p$ are shown in columns 2–4 to maximum accuracy obtainable from double-precision arithmetic. α and δ are the Feigenbaum universal exponents for index p. The capacity D (see text) of the attractors $\mathscr{A}_p$ was estimated from the slope of $\ln N(\epsilon)$ vs $\ln(1/\epsilon)$ for bin size ϵ, with ϵ between 1 and 10^{-5}, from time series up to 4×10^4 points. The information dimension σ and correlation dimension ν (Refs. 20 and 21) were estimated in the same way for the same ϵ range from 8192 points. The errors in these estimates are shown in Fig. 6.

	$-a$	$\lvert\alpha\rvert$	δ	D	σ	ν
2	1.401 155 189 092 01	2.502 908	4.669 200	0.539	0.531	0.524
2.8	1.502 954 633 550 13	2.000 000	5.822 887	0.583	0.551	0.531
4	1.594 901 356 228 81	1.690 303	7.284 698	0.630	0.543	0.520
6	1.683 260 198 204 63	1.467 756	9.296 778	0.674	0.547	0.504
8	1.736 452 374 752 32	1.358 057	10.951 105	0.683	0.539	0.465
10	1.772 643 726 066 98	1.291 584	12.348 360	0.705	0.528	0.450
12	1.799 123 137 925 2	1.246 757	13.565 497	0.744	0.522	0.441
14	1.819 465 494 920 4	1.214 072	14.597 546		0.500	0.417
16	1.835 653 773 333	1.189 346	15.560 688		0.484	0.409

tractor. Thus the attractor mass becomes concentrated near $x=\alpha^{-1}$ and 1. The flattening of M_p with increasing p is shown in Fig. 5 where 5(a) represents M_8 and 5(b) M_{16} [cf. M_4, Fig. 3(a)]. We have indicated the principal self-similar clusters of M_{16} in Fig. 5: much of the mass of this attractor is concentrated near the ends at $f_{16}(1)\cong\alpha_{16}^{-1}$ and $x=1$. For large p (>8) the attractors $\mathscr{A}_p(f)$ and $\mathscr{A}_p(g)$ are visibly different so that the b and B bounds for $\mathscr{A}_p(g)$ depart from those of $\mathscr{A}_p(f)$ by a few percent. We have looked at other p values, which confirm this flattening effect.

From the scaling properties of $\mathscr{A}_p$ a decrease in $|\alpha|$ also implies a "thickening" of attractor elements throughout $[\alpha^{-1},1]$ in the sense that the largest gap in this interval becomes arbitrarily small. These distinct effects have implications for the various dimensions characterizing these attractors. We consider, in particular, the capacity dimension[19] D,

$$D=\lim_{\epsilon\to0}\frac{\ln N(\epsilon)}{\ln(1/\epsilon)}\ ,$$

where $N(\epsilon)$ is the number of segments of length ϵ needed to cover the attractor, and the information dimension[19]

$$\sigma=\lim_{\epsilon\to0}\left[\frac{1}{\ln\epsilon}\sum_{i=1}^{N(\epsilon)}p_i\ln p_i\right]\ ,$$

where p_i is the probability of an attractor point falling in the ith segment of the partition. The capacity dimension, which depends only on the largest distance between the attractor elements, increases while the information dimension, which depends on the probability measure, decreases. $\mathscr{A}_p$ clearly becomes less homogeneous with increasing p and we might expect $\mathscr{A}_p$ to behave in a singular way at $p=\infty$. We now investigate these trends in more detail.

The large-p behavior of D and σ is partly accessible through lower-bound formulas. Grassberger[8] has shown that a first lower bound D_l to D for the attractors $\mathscr{A}_p(g)$ is given by the solution of the equation

$$\frac{1}{|\alpha|^{D_l}}+\frac{1}{|g'(1)\alpha|^{D_l}}=1\ . \tag{4.2}$$

It is easily shown that $g'(1)=-|\alpha|^{p-1}$, so that Eq. (4.2) becomes

$$\frac{1}{|\alpha|^{D_l}}+\frac{1}{|\alpha|^{pD_l}}=1\ . \tag{4.3}$$

In terms of the exponents η_c and η_e this lower-bound formula becomes

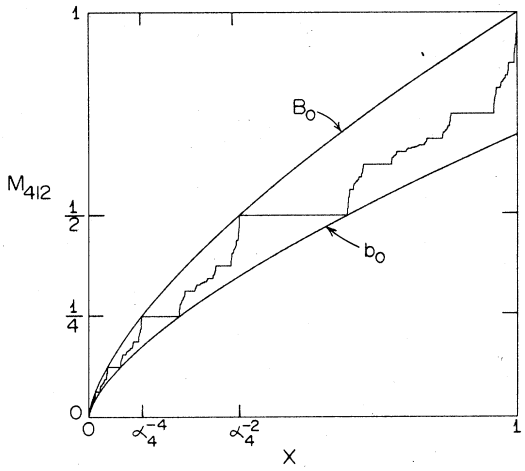

FIG. 4. Figure shows mass function $M_{4/2}(x)\equiv M(x;\mathscr{A}_{4/2})$. Global bounds b_0 and B_0 depend on intermediate quartic exponent $\eta_0=\frac{1}{2}\eta_c$. Clusters on $M_{4/2}$ scale in mass by 2^{-1} and distance by α_4^{-2} (cf. Fig. 3). Only the origin possesses scaling features with exponent η_0.

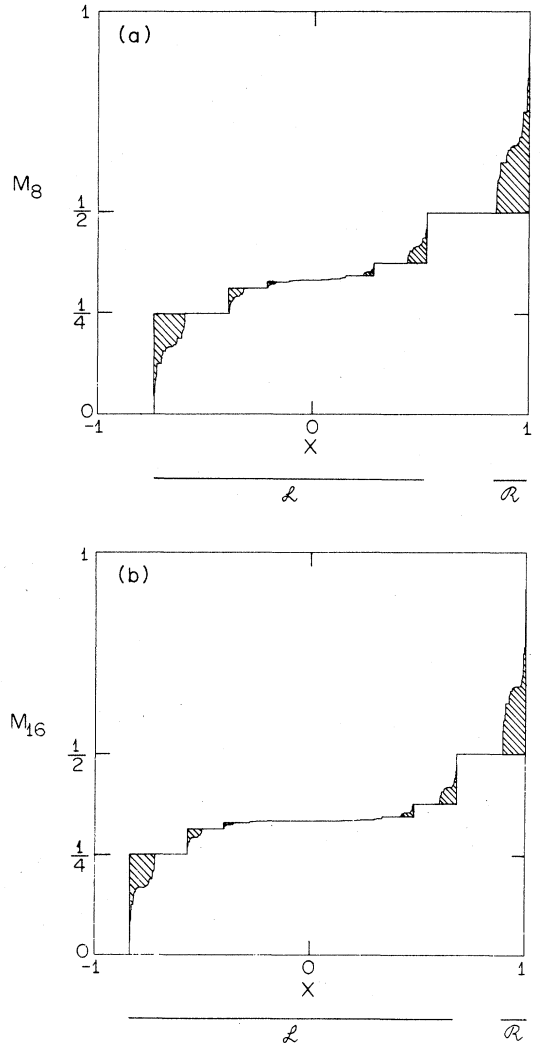

FIG. 5. (a) The mass function M_8 for $\mathscr{A}_8$. Note flatness of M_8 near $(x=0, M=\frac{1}{3})$. Half the attractor mass is contained in the interval $\mathscr{R}$ (and half in $\mathscr{L}$); $\mathscr{A}_8$ is inhomogeneous. Hatched regions indicate similar clusters scaling α_8^{-1} in width and 2^{-1} in height. Note inversion of structure to left and right of origin 0. (b) The mass curve M_{16}, which is very flat near $x=0$. $\mathscr{R}$ contains half the mass of $\mathscr{A}_{16}$. $|\alpha_{16}| \cong 1.19$ so gaps in $\mathscr{A}_{16}$ (horizontal segments on M_{16}) are not large; cf. M_p for $p<16$. Hatched regions emphasize cluster scaling as in (a).

$$2^{-D/\eta_c}+2^{-D/\eta_e}=1 , \tag{4.4}$$

which indicates the way in which D_I (or D) depends on the scaling of mass at both the center and edges of the attractor clusters.

Procaccia and Grassberger[20] give the following formula for the information dimension σ of $\mathscr{A}_p(g)$:

$$\sigma=\lim_{k\to\infty}\frac{\ln 2}{\ln|\alpha|+\frac{1}{2^{k+1}}\sum_{i=1}^{2^k}\ln|g'(x_{2i-1})|} . \tag{4.5}$$

Noting that $|g'(1)|$ is greater than any $|g'(x_{2i-1})|$ (>1) in Eq. (4.5) we obtain a lower bound σ_I to σ where

$$\sigma\geq\sigma_I(g)=\frac{2\ln 2}{(p+1)\ln|\alpha|} . \tag{4.6}$$

We note that the values of $g'(1)$ and $g(1)$ and the curvature of g imply $1-x_{-1}\gtrsim|\alpha|^{-p}$. Assuming $|\alpha|$ tends to 1, the ordering of the elements $x_4=\alpha^{-2}\leq x_3\leq x_{-1}\leq 1$ then implies that as p tends to infinity $|\alpha|^p$ also tends to infinity. Equation (4.6) then predicts that $\sigma_I(g)$ tends to zero as p tends to infinity. The expression for α in Ref. 16 confirms this conclusion. From the expression for $\eta_e=\ln 2/(p\ln|\alpha|)$ we can then write for large p

$$\sigma_I(g)\cong 2\eta_e . \tag{4.7}$$

This expression indicates the dependence of σ on the edge exponent η_e, which determines the mass clustering for large p; compare the underlying connection between σ and probability measure. Unfortunately we have not been able to construct a rigorous upper bound to σ, but estimates suggest it is zero. Heuristic arguments based on successive estimates, at decreasing ϵ, of the quotient defining σ imply that the upper bound to σ also tends to zero as p tends to infinity; however, no rigorous upper bound is available for all ϵ.

The predictions of Eq. (4.3) for D_I and (4.6) for σ_I using the α values from Table I are shown in Fig. 6 together with numerical estimates of D and σ, which are given in Table I. These results and the discussion of the dependence of D and σ on M_p suggest that $D\to 1$ and $\sigma\to 0$ as $p\to\infty$. In estimating D and σ for large p even very small values of the bin width ϵ are typically larger than the largest gap in $\mathscr{A}_p$ so that the "support" of $\mathscr{A}_p$ is effectively $[\alpha^{-1},1]$, i.e., a one-dimensional continuum, and $D=1$. But in the sum defining σ terms $p_j\ln p_j$ vanish except at $x=\alpha^{-1}\cong -1$ and $x=1$, so that at any finite resolution the probability distribution of $\mathscr{A}_p$ behaves as if it has point support: σ, which is the scaling exponent of the information entropy, vanishes.

The vanishing of σ at large p is important[21] because it suggests that $\mathscr{A}_\infty$ has a simple structure. This is evident from the singular limit of the doubling transformation Eq. (2.1) at $p=\infty$ and its corresponding attractor and orbit.

For $\alpha=-1$ no single function obeys Eq. (2.1) but we can define a pair of functions $g_\infty^{(1)}$ and $g_\infty^{(2)}$ which do and when taken together have even symmetry, like $f_\infty(x)$:

$$g_\infty^{(1)}(x)=1 \quad \text{for } x\in[-1,1),\ g_\infty^{(1)}(1)=-1$$

and (4.8)

$$g_\infty^{(2)}(-1)=-1,\ g_\infty^{(2)}(x)=1 \quad \text{for } x\in(-1,1] .$$

For $\alpha=-1$ the doubling transformation is

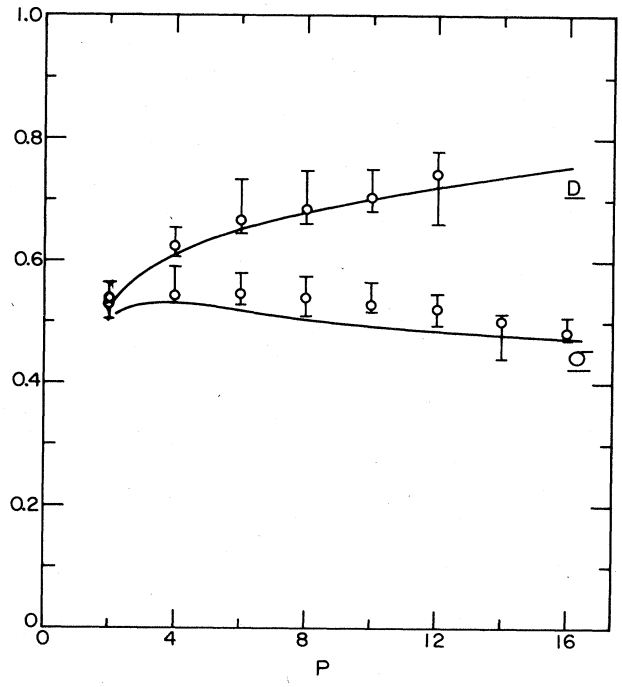

FIG. 6. Estimates of D and σ with error bars (estimated from noise in slope of binning plot). σ was obtained from 8196 points and D from up to 4×10^4 points along trajectory. Continuous curves D_l and σ_l show simplest analytical lower bounds to D and σ, which agree with numerical data.

$$-g_\infty^{(1)}(g_\infty^{(1)}(-x))=g_\infty^{(2)}(x)\ ,$$
$$-g_\infty^{(2)}(g_\infty^{(2)}(-x))=g_\infty^{(1)}(x)\ . \tag{4.9}$$

$\mathscr{A}_\infty$ under $g_\infty^{(1)}$ and $g_\infty^{(2)}$ consists of the points $x=-1$ and $x=1$. To be consistent with the limiting behavior of $M_p(x)$ for large p, $M_\infty(x)$ must have the following properties: M_∞ jumps to $\frac{1}{3}$ at $x=-1$, $M_\infty(x)=\frac{1}{3}$ for $x\in(-1,+1)$, and $M_\infty(1)=1$, i.e., a jump of $\frac{2}{3}$ at $x=1$.

This behavior of M_∞ also follows from the scaling properties of the orbit for $\alpha=-1$, i.e.,

$$x_{2j}=-x_j \text{ for all } j\ ,$$
$$x_j=1 \text{ for all odd } j\ . \tag{4.10}$$

Starting from the origin we generate from Eq. (4.8) the aperiodic orbit $\{0,+1,-1,+1,+1,+1,-1,+1,-1,\ldots\}$. The $(g_\infty^{(1)},g_\infty^{(2)})$ sequence required to generate this time series is uniquely determined. $\mathscr{A}_\infty$ thus has point support implying $\sigma=0$. However, in this singular limit $D=0$ since the orbit never revisits $(-1,+1)$, i.e., never returns to the origin. This property reflects the infinite recurrence time for return to the origin at $p=\infty$ and the exponentially large, periodic recurrence time for return to the origin at large p.

Denote the ϵ neighborhood of the origin by $\mathscr{N}_\epsilon(0)$; the recurrence time to the origin $\tau(\mathscr{N}_\epsilon(0))$ is given by

$$\tau(\mathscr{N}_\epsilon(0))=2^{-\ln\epsilon/\ln|\alpha|}\ . \tag{4.11}$$

For any $\epsilon>0$ this expression diverges as $|\alpha|\to1^+$. τ represents a periodic recurrence because at finite resolution, regions of configuration space are visited periodically.

Since $D(\mathscr{A}_\infty)=0$ this singular limit at $p=\infty$ fails (by construction) to represent the thick (almost gapless) but almost massless set in $\mathscr{A}_p$ ($p\gg1$) lying between jumps of nearly $\frac{1}{3}$ at $x=\alpha^{-1}$ and nearly $\frac{2}{3}$ at $x=1$. However, the above discussion shows how recurrence connects properties of the time series of $\mathscr{A}_p$ to its mass M_p for $p\gg1$.

V. DISCUSSION

In this paper we have examined the structure of Feigenbaum attractors $\mathscr{A}_p$ for functions in $|x|^p$ using a devil's-staircase representation of the attractor mass. Orbit scaling can be described in terms of bounds for this mass curve. Power-law conjugacy determines this global attractor scaling. It is also evident that for large p the attractor mass is very small except at the edges of its component clusters and the nonuniformity of the probability measure on $\mathscr{A}_p$ together with small separation of its elements forces the capacity D up towards 1 and the information dimension σ down to zero. The representative point on such an attractor spends most of its time at the cluster edges, only infrequently encroaching into the centers. Although the orbit is aperiodic it visits (fixed) neighborhoods of configuration space in a periodic fashion with arbitrarily long recurrence for large p.

Power-law conjugacy explains how clusters or bands of the kind just described exhibit intermediate scaling phenomena when a large-p attractor is built up from several, lower-order (quadratic) extrema. This mechanism is particularly important in dissipative flows and in the maps that imitate them: these attractors should have a sharp-edged banded appearance, i.e., a spiked probability distribution. The fact that the generalized dimensions for all attractors related by power-law conjugacy are equal generates a wide equivalence class for Feigenbaum attractors, but also shows that the set of dimensions does not completely characterize attractor structure.

Finite or banded attractors whose parameters lie close to those of $\mathscr{A}_p$ look almost fractal. For these parameters practical estimates of attractor dimension are also close to those of $\mathscr{A}_p$, thus extending its empirical importance.

The mass curve M_p displays many scaling features for $\mathscr{A}_p$ in a vivid way and demonstrates clearly connections between their structure, time evolution, and dimension.

ACKNOWLEDGMENTS

This research was supported in part by a grant from the Natural Sciences and Engineering Research Council of Canada. We would like to thank Ed Celarier for providing us with accurate data on the quartic universal function.

APPENDIX

We noted in Sec. II that the attractor $\mathscr{A}_p=\mathscr{A}_{2,1}$ and consists of a left part $\mathscr{A}_{2,4}=\mathscr{A}_L^{(0)}$ which contains the ori-

gin, and a right part $\mathscr{A}_{3,1}=\mathscr{A}_R^{(0)}$. Since these parts are mapped cyclically into one another under g each part contains half the mass, $M(\mathscr{A}_R^{(0)})=M(\mathscr{A}_L^{(0)})=\frac{1}{2}$. We call this the $j=0$ level of decimation. Clearly $\mathscr{A}_R^{(0)}$ is invariant under $g^{(2^k)}$ for $k=1,2,3,\ldots$. Next consider $\mathscr{A}_L^{(0)}$ under $g^{(2)}$ and $g^{(4)}$ at the $j=1$ level of decimation. We may write $\mathscr{A}_L^{(0)}=\mathscr{A}_L^{(1)}\cup\mathscr{A}_R^{(1)}$ where $\mathscr{A}_L^{(1)}=\mathscr{A}_{2,6}$ and $\mathscr{A}_R^{(1)}=\mathscr{A}_{8,4}$. $\mathscr{A}_L^{(1)}$ and $\mathscr{A}_R^{(1)}$ map cyclically into each other under $g^{(2)}$ and are invariant under $g^{(4)}$, thus, $M(\mathscr{A}_R^{(1)})=M(\mathscr{A}_L^{(1)})=\frac{1}{4}$. The left part is invariant under $g^{(2^k)}$ for $k=2,3,4,\ldots$ and the argument may be repeated for $\mathscr{A}_R^{(1)}$, which contains the origin. Consideration of the general case yields the following results: At the jth (j even) level of decimation the part of the attractor containing the origin is $\mathscr{A}_{2^{j+1},2^j}=\mathscr{A}_R^{(j)}\cup\mathscr{A}_L^{(j)}$ with $\mathscr{A}_L^{(j)}=\mathscr{A}_{2^{j+1},2^{j+2}}$ and $\mathscr{A}_R^{(j)}=\mathscr{A}_{2^{j+2}2^{j+1},2^j}$. $\mathscr{A}_L^{(j)}$ and $\mathscr{A}_R^{(j)}$ are mapped cyclically under $g^{(2^j)}$ and are invariant under $g^{(2^{j+1})}$, thus, $M(\mathscr{A}_R^{(j)})=M(\mathscr{A}_L^{(j)})=2^{-j-1}$. The origin now lies in $\mathscr{A}_L^{(j)}$. Similar arguments apply to the odd-j case. The part of the attractor containing the origin is $\mathscr{A}_{2^j,2^{j+1}}=\mathscr{A}_L^{(j)}\cup\mathscr{A}_R^{(j)}$ with $\mathscr{A}_L^{(j)}=\mathscr{A}_{2^j,2^{j+2}2^{j+1}}$ and $\mathscr{A}_R^{(j)}=\mathscr{A}_{2^{j+2},2^{j+1}}$. We again find for the masses $M(\mathscr{A}_L^{(j)})=M(\mathscr{A}_R^{(j)})=2^{-j-1}$. Thus, moving inward from $g(0)=1$ towards $x=0$ there are clusters of mass $\frac{1}{2},\frac{1}{8},\frac{1}{32},\ldots$ on the right of $x=0$ and these are matched by mass clusters $\frac{1}{4},\frac{1}{16},\frac{1}{64},\ldots$ on the left of the origin moving inwards from $g(1)=\alpha^{-1}$ to $x=0$. Consequently the mass on the left of the origin is $\frac{1}{3}$ while that on the right is $\frac{2}{3}$. This result is true not only for the universal function g, but for any single-extremum map supporting a Feigenbaum attractor.

[1]M. J. Feigenbaum, J. Stat. Phys. **19**, 25 (1978); **21**, 669 (1979).

[2]O. Rössler, Ann. N.Y. Acad. Sci. **79**, 6917 (1982).

[3]S. Fraser and R. Kapral, Phys. Rev. A **25**, 3223 (1982).

[4]P. Gaspard, R. Kapral, and G. Nicolis, J. Stat. Phys. **35**, 697 (1984).

[5]M. Schell, S. Fraser, and R. Kapral, Phys. Rev. A **28**, 373 (1983); P. Mandel and R. Kapral, Opt. Commun. **47**, 151 (1983).

[6]L. Glass and R. Perez, Phys. Rev. Lett. **48**, 1772 (1982); R. Perez and L. Glass, Phys. Lett. **90A**, 441 (1982); J. Belair and L. Glass, *ibid.* **96A**, 113 (1983).

[7]In order to avoid excessive notation we shall often omit the subscripts on g and M when they refer to results for arbitrary p.

[8]P. Grassberger, J. Stat. Phys. **26**, 173 (1981).

[9]See J. B. McGuire and C. J. Thompson [J. Stat. Phys. **27**, 183 (1982)] for a discussion of power-law conjugacy in relation to the doubling transformation. If attention is restricted to functions g, h, and h^{-1} defined on $x\geq 0$ then the conjugation transform is unique. However, in the present analysis it is convenient to consider functions g defined on both positive and negative x with maximum at $x=0$. In such a case one must take appropriate branches of the conjugation transformation functions so that $\mathscr{P}_q$ and its inverse preserve the correct relationship among orbit elements.

[10]P. Grassberger, Phys. Lett. **97A**, 227 (1983).

[11]There is crossover behavior at $p=2.8$ where $|\alpha|=2$ and $\eta_c=1$: the bounding curves are now straight lines. See also Table I.

[12]S. Fraser and R. Kapral, Phys. Rev. A **30**, 1017 (1984).

[13]S.-J. Chang, M. Wortis, and J. A. Wright, Phys. Rev. A **24**, 2669 (1981).

[14]R. Vilela Mendes, Phys. Lett. **84A**, 1 (1981).

[15]B. Hu and J. M. Mao, Phys. Rev. A **25**, 3259 (1982).

[16]A. Mo and P. C. Hemmer, Phys. Scr. **29**, 296 (1984).

[17]J.-P. Eckmann and P. Wittwer, C. R. Acad. Sci. **299**, 113 (1984); P. Wittwer, thesis, University of Geneva, 1984. While the limiting function considered by these authors has the same power-law behavior at the origin as the universal functions studied here and in Refs. 14—16 and 18, its shape on the entire unit interval is not the same. The behavior of α and δ in the large-p limit is different presumably for this reason.

[18]P. R. Hauser, C. Tsallis, and E. M. F. Curado, Phys. Rev. A **30**, 2074 (1984).

[19]B. Mandelbrot, *The Fractal Geometry of Nature* (Freeman, San Francisco, 1982); J. D. Farmer, Z. Naturforsch. **37A**, 1304 (1982); J. D. Farmer, E. Ott, and J. A. Yorke, Physica (Utrecht) **7D**, 153 (1983).

[20]P. Grassberger and I. Proccacia, Physica (Utrecht) D (to be published).

[21]The other generalized dimensions discussed in H. Hentschel and Proccacia [Physica (Utrecht) **8D**, 435 (1983)] also vanish in this limit.